

## ORIGINAL ARTICLE

# IFN- $\gamma$ facilitates liver fibrogenesis by CD161<sup>+</sup>CD4<sup>+</sup> T cells through a regenerative IL-23/IL-17 axis in chronic hepatitis B virus infection

Jing Li<sup>1†</sup>, Lisha Cheng<sup>2,3†</sup>, Haoyu Jia<sup>1</sup>, Chun Liu<sup>1</sup>, Siqi Wang<sup>2,4</sup>, Yun Liu<sup>2</sup>, Yue Shen<sup>2,4</sup>, Shengdi Wu<sup>2,4</sup>, Fanli Meng<sup>5</sup>, Beishi Zheng<sup>6</sup>, Changqing Yang<sup>1</sup> & Wei Jiang<sup>2,4,7</sup>

<sup>1</sup>Department of Gastroenterology and Hepatology, Tongji Hospital, School of Medicine, Tongji University, Shanghai, China

<sup>2</sup>Department of Gastroenterology and Hepatology, Zhongshan Hospital, Fudan University, Shanghai, China

<sup>3</sup>Department of Oncology, Xiamen Branch of Zhongshan Hospital, Fudan University, Shanghai, China

<sup>4</sup>Shanghai Institute of Liver Disease, Shanghai, China

<sup>5</sup>Department of Hepatology, Qilu Hospital, Shandong University, Shandong, China

<sup>6</sup>Department of Internal Medicine, Woodhull Medical Center, New York, NY, USA

<sup>7</sup>Department of Gastroenterology and Hepatology, Xiamen Branch of Zhongshan Hospital, Fudan University, Shanghai, China

## Correspondence

C Yang, Department of Gastroenterology and Hepatology, Tongji Hospital, School of Medicine, Tongji University, 389 Xincun Road, Putuo District, 200065, Shanghai, China.

Email: cqyang@tongji.edu.cn

W Jiang, Department of Gastroenterology and Hepatology, Zhongshan Hospital, Fudan University, 180 Fenglin Road, Xuhui District, 200032, Shanghai, China.

Email: jiang.wei@zs-hospital.sh.cn

<sup>†</sup>Equal contributors.

Received 16 February 2021;

Revised 1 October 2021;

Accepted 11 October 2021

doi: 10.1002/cti.1353

*Clinical & Translational Immunology*  
2021; 10: e1353

## Abstract

**Objectives.** This study aimed to determine the role of CD161<sup>+</sup>CD4<sup>+</sup> T cells in chronic hepatitis B virus (HBV) infection. **Methods.** A total of 94 patients with chronic hepatitis B (CHB), 73 with liver cirrhosis (LC) and 28 healthy controls were enrolled to determine frequency, cytokine production and chemokine receptor expression of circulating CD161<sup>+</sup>CD4<sup>+</sup> T cells. Among these, 50 CHB and 34 LC patients were followed up for a period of 52-week entecavir monotherapy to assess the association of CD161<sup>+</sup>CD4<sup>+</sup> T cells with seroconversion of HBV e antigen (HBeAg). In addition, 15 patients with hepatocellular carcinoma (HCC) and 15 with hepatic haemangioma (HHA) were enrolled to compare the paired circulating and intrahepatic CD161<sup>+</sup>CD4<sup>+</sup> T cells. **Results.** CD161<sup>+</sup>CD4<sup>+</sup> T cells were found to accumulate in the circulation of HBV cohorts, which showed a significant correlation with the clinical parameters of disease progression. In addition, higher numbers of circulating CD161<sup>+</sup>CD4<sup>+</sup> T cells were associated with an improved serological response of HBeAg to antiviral treatment. Moreover, CD161<sup>+</sup>CD4<sup>+</sup> T cells as compared to homologous CD161<sup>-</sup>CD4<sup>+</sup> T cells produced more pro-inflammatory cytokines including interleukin (IL)-17 and interferon (IFN)- $\gamma$  and expressed higher levels of liver-homing chemokine receptors including CCR6, CXCR6 and CX3CR1. Notably, a significant enrichment of CD161<sup>+</sup>CD4<sup>+</sup> T cell subsets co-expressing IFN- $\gamma$  and IL-17 was observed in HBV-associated cirrhotic livers. During *in vitro* co-cultures, circulating CD161<sup>+</sup>CD4<sup>+</sup> T cells in the chronic HBV setting exhibited prominent pro-fibrogenic effects by regulating primary hepatic stellate cells through a regenerative IFN- $\gamma$ /IL-23/IL-17 axis. **Conclusions.** In chronic HBV infection, CD161<sup>+</sup>CD4<sup>+</sup> T cells play antiviral, pro-inflammatory and pro-fibrogenic roles.

**Keywords:** CD161<sup>+</sup>CD4<sup>+</sup> T cells, interferon- $\gamma$ , interleukin 17, liver fibrosis, HBV

## INTRODUCTION

Despite the global vaccination policies for hepatitis B virus (HBV), the incidence of mortality from liver cirrhosis (LC) and hepatocellular carcinoma (HCC) associated with this virus continues to increase around the world. During chronic HBV infection, persistent immune-mediated liver damage is a well-established driving force of liver fibrogenesis and carcinogenesis. Although the underlying mechanisms are yet to be fully understood, recently, CD4<sup>+</sup> T cells have been found to play a role.<sup>1</sup>

Originally a marker of natural killer (NK) cells, the C-type lectin CD161 was subsequently identified in T cells. In the last decade, a number of studies have elucidated the role of CD161 signalling in infectious and inflammatory diseases. First, it is critical to control the virus, since CD161 expression is not only enriched in HBV- and HCV-specific CD8<sup>+</sup> T cells,<sup>2,3</sup> but also documented on mucosal-associated invariant T (MAIT) cells, which could co-express invariant TCR V $\alpha$ 7.2, and have recently been characterised to have antiviral effects.<sup>4,5</sup> Second, CD161 expression on T cells has been linked with a pattern of molecules suggesting type 17 differentiation, including cytokines [interleukin (IL)-17, IL-22], cytokine receptors (IL-23R, IL-18R) and liver-homing chemokine receptors (CCR6, CXCR6).<sup>3,6</sup> Third, as a co-stimulatory receptor, CD161 endows T cells with the innate ability to produce interferon (IFN)- $\gamma$  in response to IL-12 and IL-18, which is independent of antigen recognition by the T-cell receptor.<sup>2,7</sup> Current knowledge of CD161 signalling in chronic hepatitis B (CHB) has been mainly obtained from CD161<sup>+</sup>CD8<sup>+</sup> T cells; however, the role of CD161<sup>+</sup>CD4<sup>+</sup> T cells in chronic HBV infection is yet to be determined.

As the cornerstone of liver fibrosis progression, quiescent hepatic stellate cells (HSCs) activate and transform into myofibroblast-like cells, which produce a large amount of extracellular matrix, such as collagen type I, and pro-fibrogenic cytokines, such as transforming growth factor

(TGF) and platelet-derived growth factor (PDGF).<sup>8</sup> Intriguingly, activated HSCs behave like antigen-presenting cells (APCs) and regulate T-cell responses.<sup>9,10</sup> A wealth of studies<sup>11–13</sup> and our previous work<sup>14–16</sup> have attempted to bridge intrahepatic inflammation and fibrosis pathways by exploring the cellular crosstalk between immune cells and HSCs. Although CD161<sup>+</sup>CD4<sup>+</sup> T cells can produce abundant IFN- $\gamma$  and IL-17, both of which play a role in liver fibrogenesis,<sup>4,17</sup> There are no available data on CD161<sup>+</sup>CD4<sup>+</sup> T cells in liver fibrosis.

Taking advantage of a large HBV cohort, this study extensively characterised circulating and intrahepatic CD161<sup>+</sup>CD4<sup>+</sup> T cells in terms of cytokine production and chemokine receptor expression and explored their associations with HBV-related disease parameters. These findings could greatly expand our knowledge about the role of CD161<sup>+</sup>CD4<sup>+</sup> T cells in HBV-mediated pathogenesis.

## RESULTS

### Accumulation of circulating CD161<sup>+</sup>CD4<sup>+</sup> T cells in HBV cohorts

The association between CD161<sup>+</sup>CD4<sup>+</sup> T cells and HBV-related disease parameters has not been investigated previously. Here, using the gating strategy shown in Figure 1a, the frequencies of circulating CD161<sup>+</sup>CD4<sup>+</sup> T cells were determined in different HBV cohorts. First, a significant accumulation of CD161<sup>+</sup>CD4<sup>+</sup> T cells was documented in the circulation of CHB and LC compared with the HC group (Figure 1b and c). Second, higher frequencies of CD161<sup>+</sup>CD4<sup>+</sup> T cells were detected in HBeAg<sup>-</sup> than in HBeAg<sup>+</sup> patients with CHB (Figure 1d). Third, the frequencies increased along with more advanced scores of intrahepatic inflammation and fibrosis in the biopsied HBV cohort (Figure 1e). Intriguingly, there was a closer correlation of the frequencies with HBV-related disease parameters in HBeAg<sup>-</sup> than in HBeAg<sup>+</sup> patients with CHB (Figure 1f), being positive for ALT or liver stiffness, negative

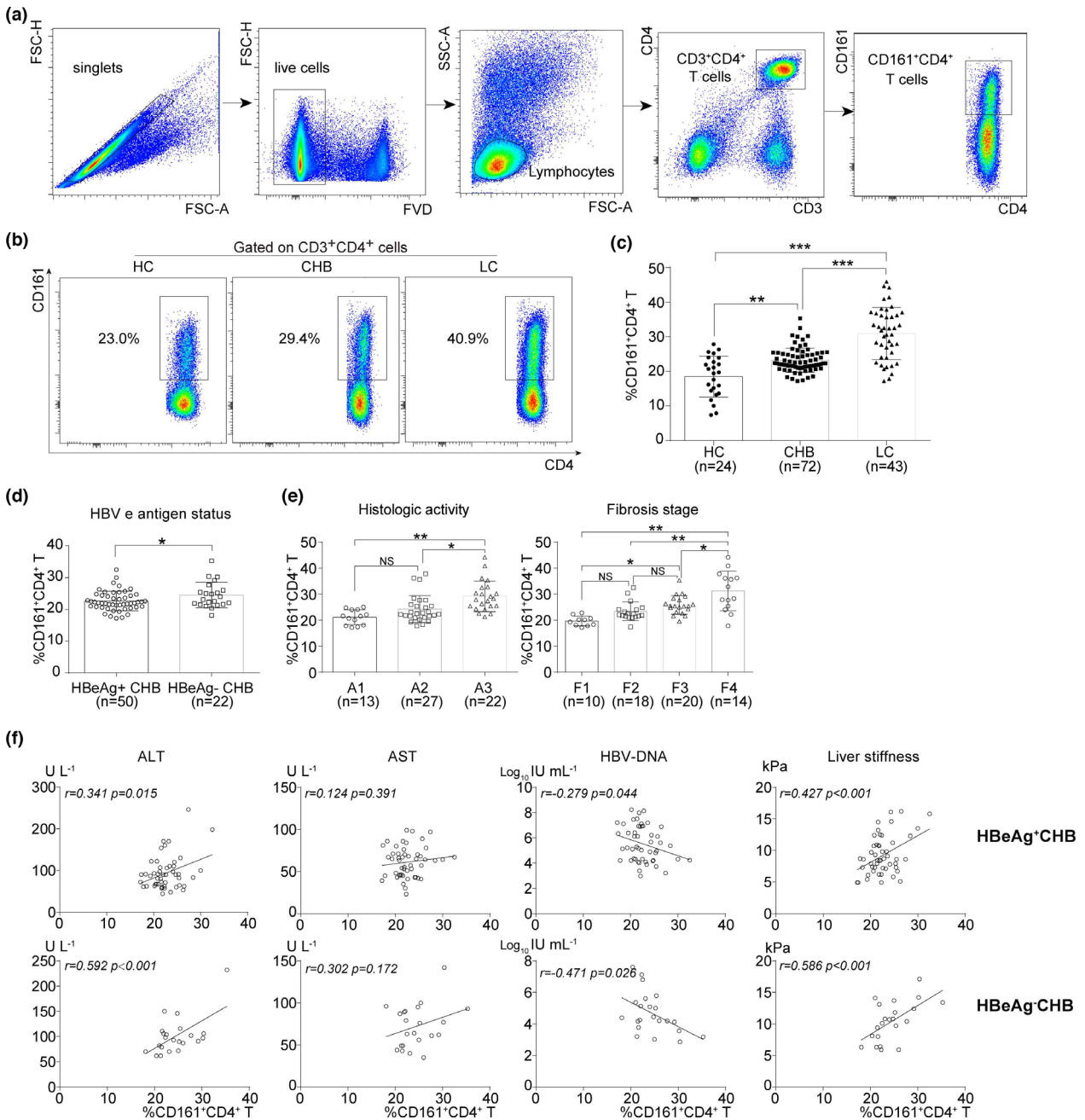


**Figure 1.** Accumulation of circulating CD161<sup>+</sup>CD4<sup>+</sup> T cells in HBV cohorts. **(a)** Gating strategy for CD161<sup>+</sup>CD4<sup>+</sup> T cells (FSC, forward scatter; SSC, side scatter). **(b, c)** Representative scatter plots **(b)** and statistical analysis of frequencies **(c)** of circulating CD161<sup>+</sup>CD4<sup>+</sup> T cells in HC, CHB and LC groups. **(d, e)** Statistical analysis of circulating CD161<sup>+</sup>CD4<sup>+</sup> T cell frequencies in CHB patients classified with HBeAg statuses **(d)** or in biopsy HBV cohort classified with Metavir scores **(e)**. **(f)** Statistical correlations of circulating CD161<sup>+</sup>CD4<sup>+</sup> T cell frequencies were performed with the levels of ALT, AST, HBV DNA or liver stiffness, in HBeAg<sup>+</sup> and HBeAg<sup>-</sup> CHB patients, respectively (\**P* < 0.05; \*\**P* < 0.01; \*\*\**P* < 0.001; NS, not significant).

for HBV DNA and not significant for AST. Unexpectedly, the statistical analysis of the LC cohort based on disease parameters including

Child Pugh score, HBeAg status and HBV DNA yielded no significant findings (Supplementary figure 1a–c).

### Higher frequencies of circulating CD161<sup>+</sup>CD4<sup>+</sup> T cells are associated with increased HBeAg seroconversion in HBeAg<sup>+</sup> patients undergoing antiviral treatment

Treatment-induced HBeAg seroconversion represents a partial immune control of chronic HBV infection and is associated with a reduced risk of disease progression. Here, the role of CD161<sup>+</sup>CD4<sup>+</sup> T cells in HBeAg seroconversion was determined using a longitudinal cohort of HBeAg<sup>+</sup> patients (containing 50 CHB and 34 LC) who had achieved HBeAg seroconversion (responders) or not (non-responders) after a period of 52-week antiviral treatment with entecavir. Notably, responders had significantly higher baseline frequencies in both the CHB (Figure 2a) and LC (Supplementary figure 1d) groups compared to non-responders. However, the serial data (at treatment weeks 0 and 52) of responders only documented a significant increase

in circulating CD161<sup>+</sup>CD4<sup>+</sup> T frequencies in CHB (Figure 2b) rather than in the LC (Supplementary figure 1e) group. In addition, based on the mean value of baseline frequencies, we divided CHB and LC (Supplementary figure 1f, h) groups into 'low' and 'high' subgroups, respectively, and found that the responder rate was much higher in the 'high' subgroup ('high' vs. 'low', CHB: 42.11% vs. 9.68%, LC: 27.78% vs. 6.25%). Meanwhile, ROC curves were generated using CHB and LC (Supplementary figure 1g, i) data, demonstrating the statistical value of the baseline frequency to predict HBeAg seroconversion at week 52 (AUC = 0.784, *P* = 0.004). Moreover, the expression of markers of exhaustion (CD39, PD-1, CTLA-4 and Tim-3) and proliferation (Ki-67) was determined in circulating CD161<sup>+</sup>CD4<sup>+</sup> T cells. Serial data documented a decreased exhaustion with an enhanced proliferation of cells from responders; however, there were no significant findings in non-responders (Figure 2c and d).

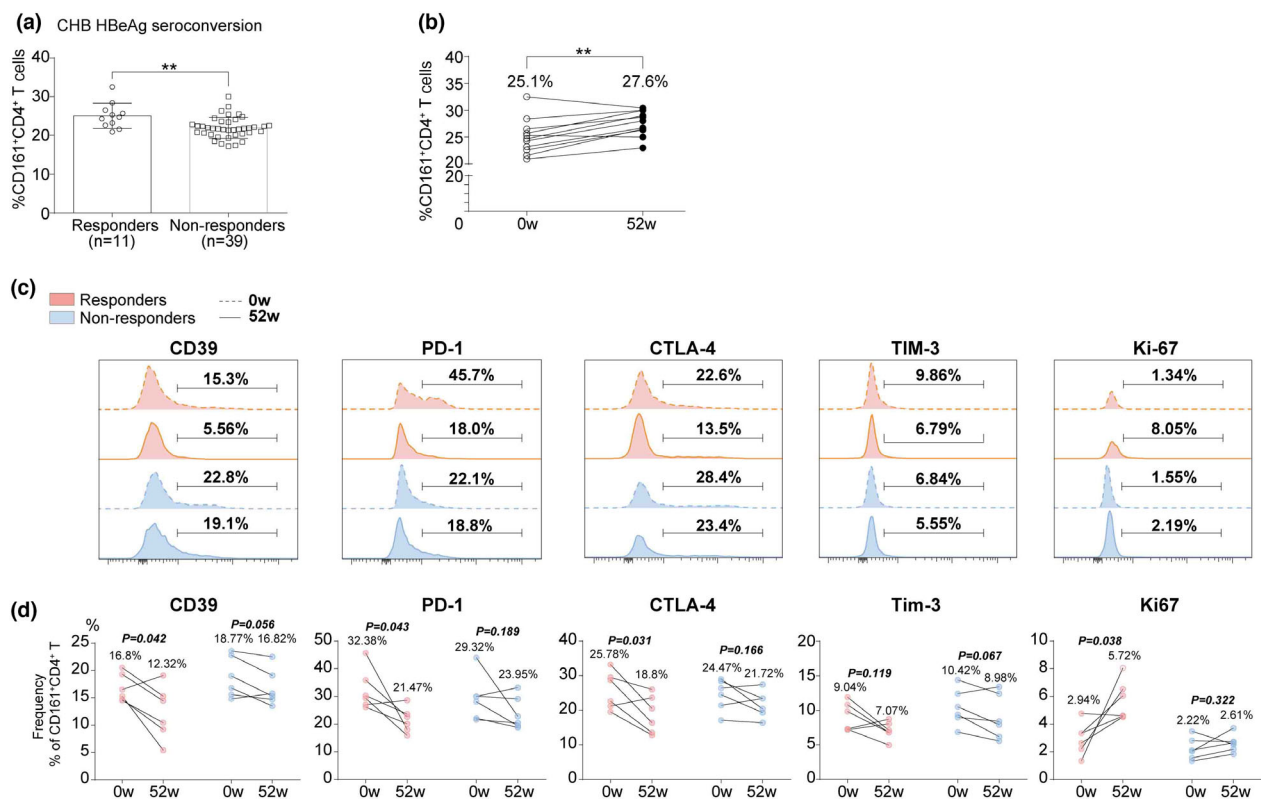


**Figure 2.** Increased circulating CD161<sup>+</sup>CD4<sup>+</sup> T cell frequencies correlate with improved serological responses of HBeAg to antiviral treatment. **(a)** In the CHB group, responders as compared to non-responders had much higher baseline frequencies of circulating CD161<sup>+</sup>CD4<sup>+</sup> T cells. **(b)** Serial changes (week 0 and week 52 after entecavir therapy) of circulating CD161<sup>+</sup>CD4<sup>+</sup> T cell frequencies in CHB responders (*n* = 11). **(c, d)** Serial changes of ex vivo expression of markers of exhaustion (CD39, PD-1, CTLA-4 and TIM-3) and proliferation (Ki-67) by circulating CD161<sup>+</sup>CD4<sup>+</sup> T cells from CHB responders and non-responders (both *n* = 6) (\*\**P* < 0.01).

**Phenotypic analysis of circulating CD161<sup>+</sup>CD4<sup>+</sup> T and homologous CD161<sup>-</sup>CD4<sup>+</sup> T cells from patients with CHB**

Using peripheral blood mononuclear cells (PBMCs) from patients with CHB (*n* = 18), the phenotypic analysis of CD161<sup>+</sup>CD4<sup>+</sup> T cells was first carried out by the flow cytometric co-staining of CD4/CD161 with the following indicators: intracellular cytokines (pro-inflammatory IFN- $\gamma$ , IL-17A, TNF- $\alpha$ , IL-22 and anti-inflammatory IL-4 and IL-10) and membrane proteins (Foxp3, the lineage-specific transcription factor of regulatory T cells; CD25, a T-cell activation marker; CD45RO, an immune memory marker). Statistical data indicated that CD161<sup>+</sup>CD4<sup>+</sup> T vs. CD161<sup>-</sup>CD4<sup>+</sup> T cells expressed

much higher levels of IFN- $\gamma$ , IL-17A, TNF- $\alpha$  and CD45RO, along with similar levels of IL-22, IL-10, IL-4, Foxp3 and CD25, displaying a pro-inflammatory and memory-like phenotype (Figure 3a and b). In addition, data documented a significant liver-homing ability of CD161<sup>+</sup>CD4<sup>+</sup> T vs. CD161<sup>-</sup>CD4<sup>+</sup> T cells, as reflected by the much higher expression levels of chemokine receptors, including CCR6, CXCR6 and CX3CR1 (Figure 3c and d).

To explore the role of CD161 signalling in CD4<sup>+</sup> T cells, sorted CD161<sup>+</sup>CD4<sup>+</sup> T cells from the circulation of patients with CHB (*n* = 10) were treated for 72 h with or without imipramine (the inhibitor of CD161 signalling via suppression of acid sphingomyelinase (ASM)),<sup>17</sup> anti-CD161 Ab (the activator of CD161 signalling) or recombinant IL-23 (rIL-23, the

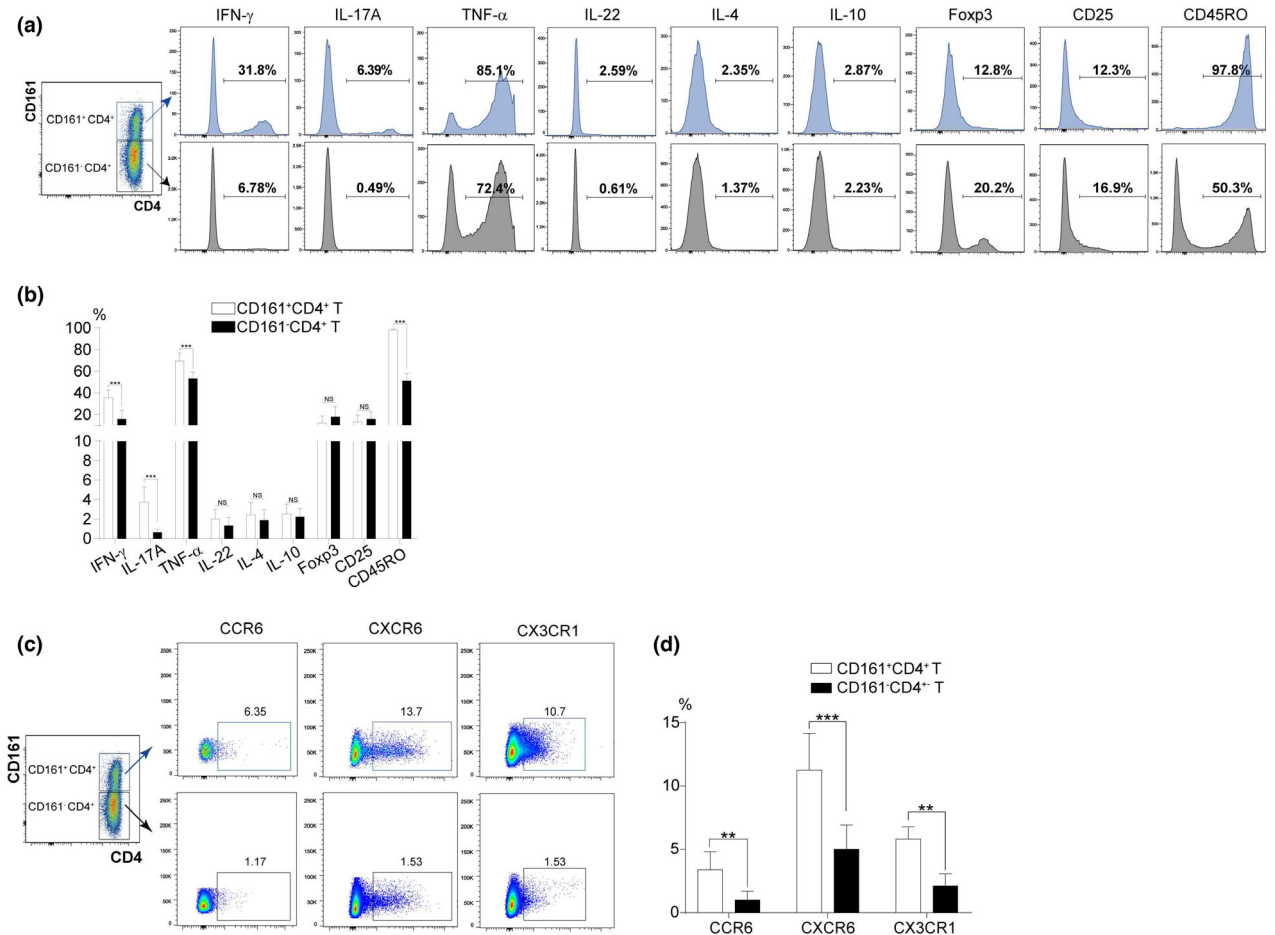


**Figure 3.** Phenotypic comparison between circulating CD161<sup>+</sup>CD4<sup>+</sup> T cells and homologous CD161<sup>-</sup>CD4<sup>+</sup> T cells from patients with CHB. **(a, b)** Representative histograms **(a)** and statistical analysis of frequencies **(b)** of IFN- $\gamma$ , IL-17A, TNF- $\alpha$ , IL-22, IL-4, IL-10, Foxp3, CD25 or CD45RO expressing CD4<sup>+</sup> T cells according to CD161 expression in the CHB group (*n* = 18). **(c, d)** Representative pseudocolour plots **(c)** and statistical analysis of frequencies **(d)** of CCR6, CXCR6 or CX3CR1 expressing CD161<sup>+</sup>CD4<sup>+</sup> T cells and CD161<sup>-</sup>CD4<sup>+</sup> T cells from patients with CHB (*n* = 16) (\*\**P* < 0.01; \*\*\* *P* < 0.001; NS, not significant).

upstream signal of Th17 differentiation).<sup>18,19</sup> Cytometric beads array (CBA) analysis demonstrated that imipramine significantly decreased the *in vitro* production of IFN- $\gamma$ , IL-17A, TNF- $\alpha$  and IL-22 by CD161<sup>+</sup>CD4<sup>+</sup> T cells rather than CD161<sup>-</sup>CD4<sup>+</sup> T cells (Supplementary figure 2b). Furthermore, imipramine downregulated and anti-CD161 Ab or rIL-23 upregulated the activation/phosphorylation level of STAT3 (a transcription factor associated with IL-17 production) in CD161<sup>+</sup>CD4<sup>+</sup> T cells and the supernatant concentration of IL-17 (Supplementary figure 2c–e).

### **Circulating CD161<sup>+</sup>CD4<sup>+</sup> T cells in HBV cohorts express a pattern of cytokines and liver-homing chemokine receptors**

The expression of CD161 in T cells is closely linked with the production of IFN- $\gamma$  and IL-17, both of which play a role in liver inflammation and fibrosis. Thus, we next focused on analysing IFN- $\gamma$ /IL-17 or liver-homing receptors expressing CD161<sup>+</sup>CD4<sup>+</sup> T cell subsets in the circulation. First, we found that IL-17<sup>+</sup>, IFN- $\gamma$ <sup>+</sup> and IL-17<sup>+</sup>IFN- $\gamma$ <sup>+</sup> subsets were significantly increased in the CHB and LC groups, with the most dramatic changes detected in IL-17<sup>+</sup>IFN- $\gamma$ <sup>+</sup> subsets (Figure 4a and b), which also significantly increased with more advanced histological scores (Figure 4c). Second, we observed that CCR6, CXCR6 or CX3CR1 expressing subsets accumulated not only in the CHB and LC groups (Figure 4d and e), but also in the biopsied HBV cohort with elevated histological scores (Figure 4f). Third, we roughly quantified the intrahepatic CD161<sup>+</sup> cells (containing T, NK and MAIT) in liver biopsy samples by immunohistochemical staining and documented a significant increase in the cell number along with more advanced histological scores (Figure 4g and h). Moreover, we established positive correlations between the intrahepatic CD161<sup>+</sup> cell number and frequencies of peripheral CCR6, CXCR6 or CX3CR1 expressing CD161<sup>+</sup>CD4<sup>+</sup> T cell subsets, using paired data analysis (Figure 4i), suggesting liver recruitment as a possible way to expand intrahepatic CD161<sup>+</sup> cells in disease conditions.

### **Associations between circulating and intrahepatic CD161<sup>+</sup>CD4<sup>+</sup> T cells in HBV-mediated cirrhosis**

To dissect the potential associations between circulating and intrahepatic CD161<sup>+</sup>CD4<sup>+</sup> T cells in

chronic HBV setting, paired (blood and liver) specimens were collected from HHA (normal) and HCC (cirrhotic) cohorts for subsequent flow cytometric analysis. Initially, an enrichment of total CD161<sup>+</sup>CD4<sup>+</sup> T cells was observed in cirrhotic livers, despite poor correlations between the paired cell frequencies (Figure 5a). Notably, CD161<sup>+</sup>CD4<sup>+</sup> T cell subsets co-expressing IL-17 and IFN- $\gamma$  were enriched in cirrhotic livers, with a positive correlation between the paired subset frequencies (Figure 5b). Moreover, although a similar enrichment of CD161<sup>+</sup>CD4<sup>+</sup> T cell subsets expressing CCR6, CXCR6 or CX3CR1 was detected in cirrhotic livers, the positive correlations between the paired subset frequencies were only established in CCR6<sup>+</sup> and CXCR6<sup>+</sup> instead of the CX3CR1<sup>+</sup> subset (Figure 5c and d). These findings collectively indicate that circulating CD161<sup>+</sup>CD4<sup>+</sup> T cell subsets that co-express IL-17/IFN- $\gamma$ , CCR6 or CXCR6 may greatly contribute to the increased number of their intrahepatic counterparts through liver infiltration.

### **Intrahepatic chemokine expression for circulating CD161<sup>+</sup>CD4<sup>+</sup> T cells in HBV-mediated cirrhosis**

The tissue-homing process is triggered by the interaction between chemokines and chemokine receptors. To obtain more direct evidence of liver infiltration of circulating CD161<sup>+</sup>CD4<sup>+</sup> T cells, immunohistochemistry was performed to determine intrahepatic chemokine expression and observe spatial contacts with CD161<sup>+</sup> cells. First, statistical data documented the increased chemokine expression of CCL20, CXCL16, and CX3CL1, the respective ligands for chemokine receptors, including CCR6, CXCR6, and CX3CR1, in cirrhotic livers (Figure 6a and b). Next, the increased number of CD161<sup>+</sup>CD4<sup>+</sup> T cells was confirmed in cirrhotic livers by double staining of CD161 and CD4 (Figure 6c). In addition, positive correlations were established especially in cirrhotic conditions between the intrahepatic CD161<sup>+</sup>CD4<sup>+</sup> T cell number and chemokine expression (including CCL20,  $r = 0.59$ ; CXCL16,  $r = 0.62$ ; CX3CL1,  $r = 0.53$ ) (Figure 6d). Moreover, the intrahepatic expression of CD161 not only increased with enhanced chemokine expression in cirrhotic livers, but also exhibited a close proximity with each chemokine in spatial position, as reflected by double staining of CD161 and CCL20, CD161 and CXCL16, or CD161 and CX3CL1 (Figure 6e).

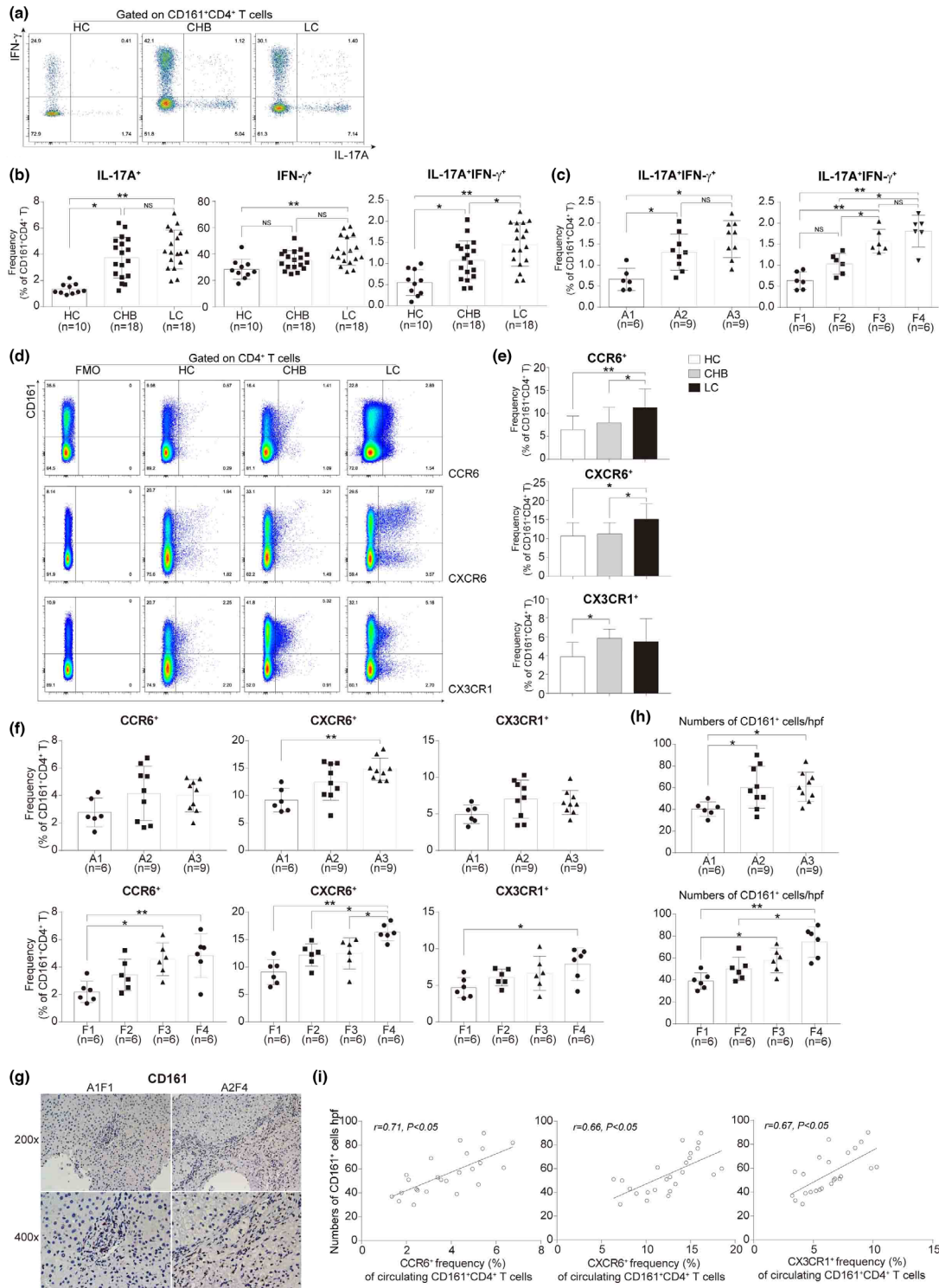


**Figure 4.** Circulating CD161<sup>+</sup>CD4<sup>+</sup> T cells of HBV cohorts express a certain pattern of cytokines and liver-homing chemokine receptors. **(a, b)** Representative scatter plots **(a)** and statistical analysis of frequencies **(b)** of IL-17A, IFN- $\gamma$  or IL-17A/IFN- $\gamma$  producing CD161<sup>+</sup>CD4<sup>+</sup> T cell subsets in HC, CHB and LC groups. **(c)** Statistical analysis of frequencies of IL-17A/IFN- $\gamma$  co-producing CD161<sup>+</sup>CD4<sup>+</sup> T cell subsets in the biopsied HBV cohort. **(d-f)** Representative scatter plots **(d)** and statistical analysis of frequencies **(e, f)** of CCR6, CXCR6 or CX3CR1 expressing CD161<sup>+</sup>CD4<sup>+</sup> T cell subsets in HC, CHB and LC groups (all  $n = 24$ ) **(e)**, and in the biopsied HBV cohort **(f)**. **(g-i)** Representative immunohistochemical staining **(g)** and quantification **(h)** of intrahepatic CD161<sup>+</sup> cells (hpf, high-power field, 400 $\times$  magnification) in the biopsied HBV cohort. **(i)** Statistical correlations between the intrahepatic CD161<sup>+</sup> T cell number and frequencies of circulating CD161<sup>+</sup>CD4<sup>+</sup> T cell subsets expressing CCR6, CXCR6 or CX3CR1 in the biopsied HBV cohort (\* $P < 0.05$ ; \*\* $P < 0.01$ ).

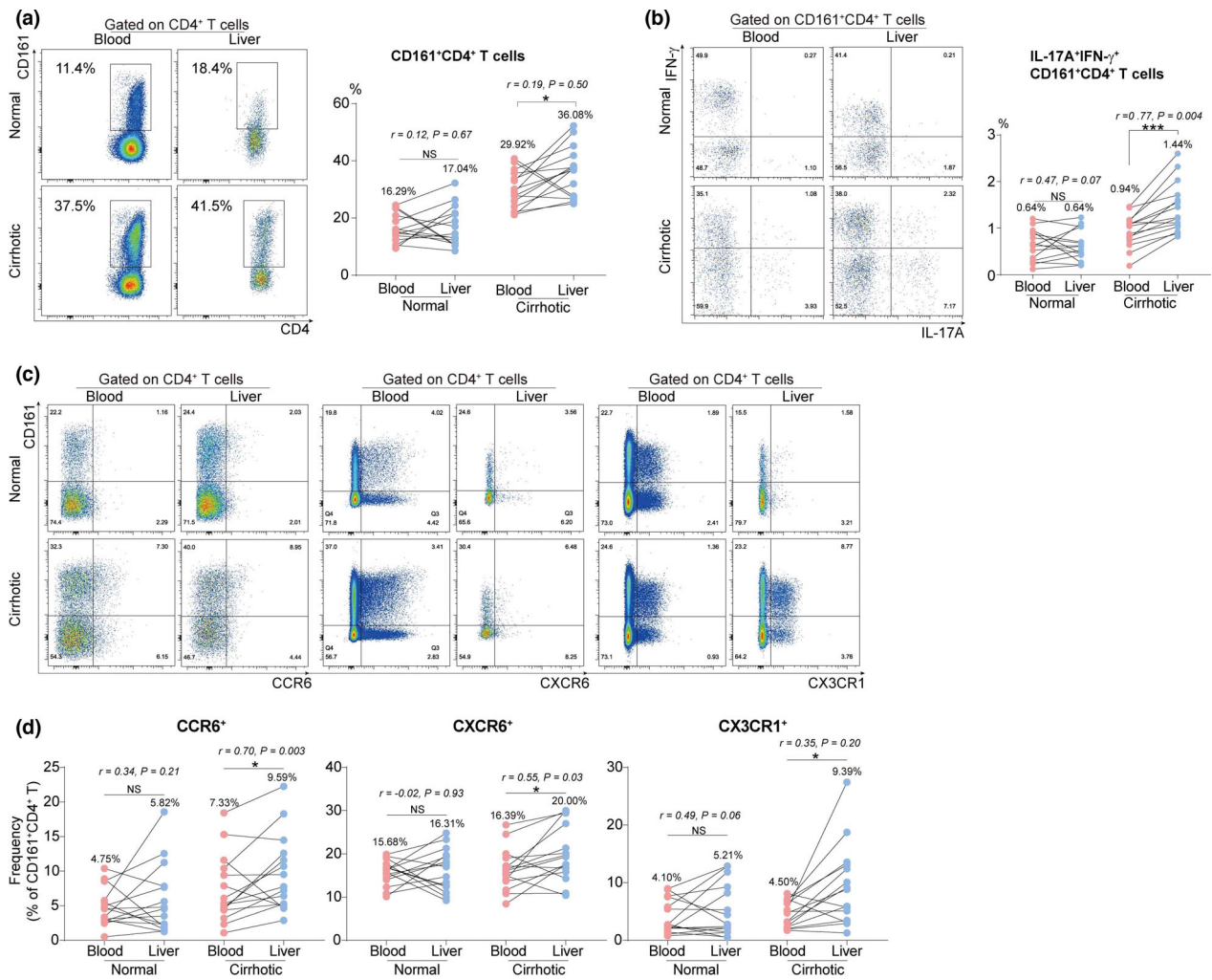


**Figure 5.** Associations between circulating and intrahepatic CD161<sup>+</sup>CD4<sup>+</sup> T cells in HBV-mediated cirrhosis. **(a)** Representative scatter plots (left panel) and statistical analysis of frequencies (right panel) of the paired (circulating and intrahepatic) CD161<sup>+</sup>CD4<sup>+</sup> T cells in HHA and HCC cohorts (labelled as normal and cirrhotic, respectively, both  $n = 15$ ). **(b)** Representative scatter plots (left panel) and statistical analysis of frequencies (right panel) of the paired CD161<sup>+</sup>CD4<sup>+</sup> T cell subsets producing IL-17/IFN- $\gamma$  in HHA and HCC cohorts. **(c, d)** Representative scatter plots **(c)** and statistical analysis of frequencies **(d)** of the paired CD161<sup>+</sup>CD4<sup>+</sup> T cell subsets expressing CCR6, CXCR6 or CX3CR1 in HHA and HCC cohorts (\* $P < 0.05$ ; \*\*\* $P < 0.001$ ; NS, not significant).

### The pro-fibrogenic features of circulating CD161<sup>+</sup>CD4<sup>+</sup> T cells in chronic HBV setting

In this part of the study, the effects of circulating CD161<sup>+</sup>CD4<sup>+</sup> T cells in liver fibrosis were determined after *in vitro* co-cultures with pHSCs, which were then collected for analysis of the well-established genes in liver fibrogenesis, including  $\alpha$ -SMA, collagen type I, TGF- $\beta$ 1 and tissue inhibitor of metalloproteinase 1 (TIMP1). To begin with, in contact co-cultures, LC rather than CHB-sourced CD161<sup>+</sup>CD4<sup>+</sup> T cells, at a cell ratio of 1:1 with pHSCs, were found to have pro-fibrogenic effects

(Supplementary figure 4c, d). Subsequent co-cultures were conducted using CD161<sup>+</sup>CD4<sup>+</sup> T cells from the LC cohort at a cell ratio of 1:1. After co-culturing pHSCs with homologous CD161<sup>+</sup>CD4<sup>+</sup> T or CD161<sup>+</sup>CD4<sup>+</sup> T cells in the contact or transwell (non-contact) manner, CD161<sup>+</sup>CD4<sup>+</sup> T cells rather than CD161<sup>+</sup>CD4<sup>+</sup> T cells exhibited pro-fibrogenic effects in both manners, which were much more remarkable in the contact manner, suggesting a role for membrane proteins in direct cell contacts (Figure 7a). CD161<sup>+</sup>CD4<sup>+</sup> T cells can produce both anti-fibrotic IFN- $\gamma$  and pro-fibrotic IL-17, and IL-23 is an important trigger of IL-17 production by



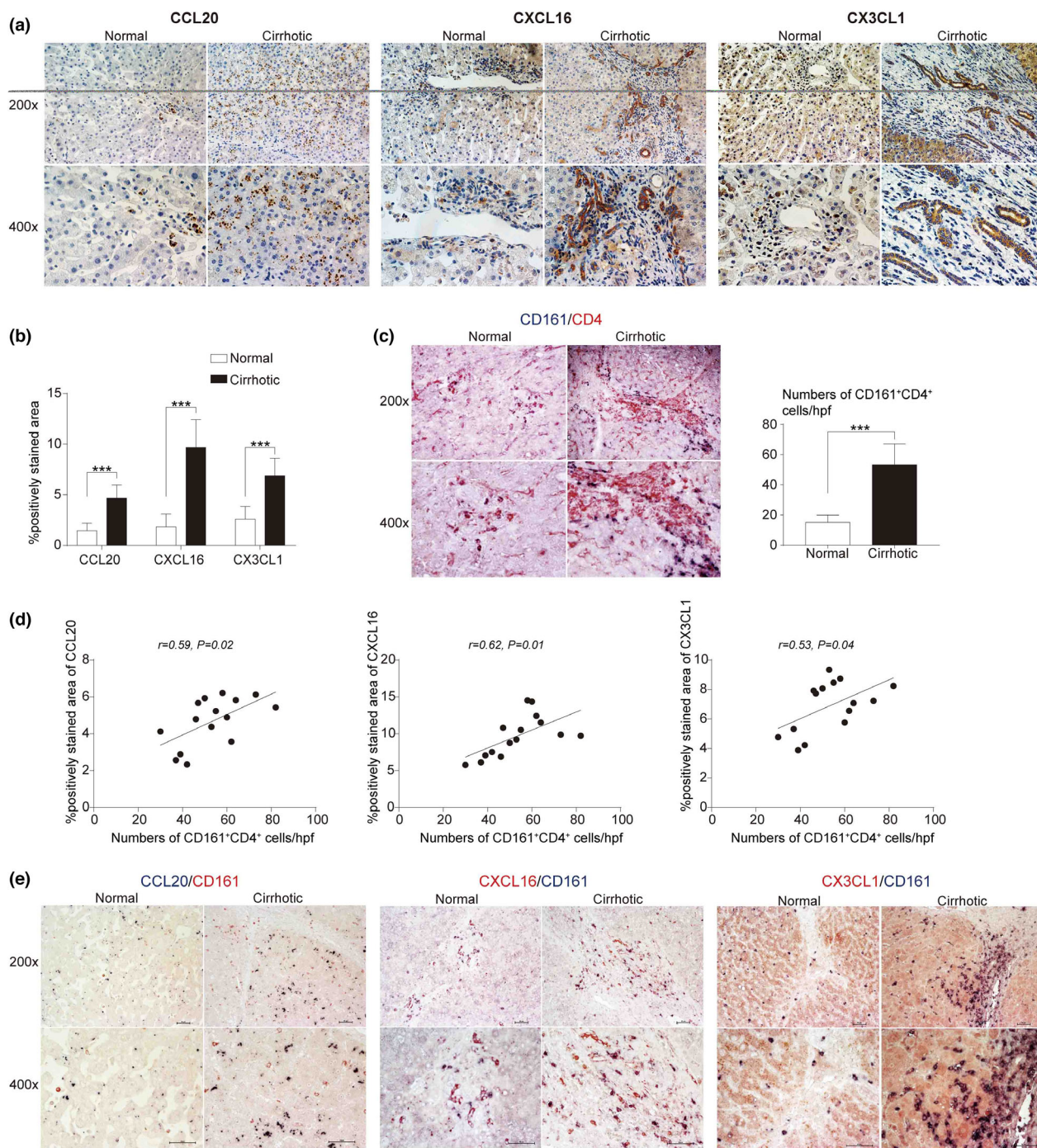


**Figure 6.** Intrahepatic chemokine expression for circulating CD161<sup>+</sup>CD4<sup>+</sup> T cells in HBV-mediated cirrhosis. **(a, b)** Representative immunohistochemical staining **(a)** and quantification of expression **(b)** of intrahepatic chemokines CCL20, CXCL16 and CX3CL1 (ligands for CCR6, CXCR6 and CX3CR1, respectively) in HHA and HCC cohorts (both  $n = 15$ ). **(c)** Representative immunohistochemical co-staining of CD4 (red)/CD161(blue) (left panel) and quantification of intrahepatic CD161<sup>+</sup>CD4<sup>+</sup> T cell numbers (right panel). **(d)** Statistical correlations of liver-infiltrating CD161<sup>+</sup>CD4<sup>+</sup> T cells, respectively, with intrahepatic expression of CCL20, CXCL16 and CX3CL1 in HCC cohort ( $n = 15$ ). **(e)** Representative immunohistochemical co-staining of intrahepatic CD161/CCL20, CD161/CXCL16 or CD161/CX3CL1 in HHA and HCC cohorts ( $n = 6$ ) ( $***P < 0.001$ ).

IL-23R<sup>+</sup>CD161<sup>+</sup>CD4<sup>+</sup> T subsets.<sup>18,19</sup> Thus, IL-17, IFN- $\gamma$  and IL-23 were suspected to formulate a functional axis to regulate liver fibrogenesis, which was then explored with the assistance of neutralising anti-IL-17, anti-IL-23 and anti-IFN- $\gamma$  Abs. In the transwell assay, only the neutralisation of IL-17 significantly inhibited liver fibrogenesis, demonstrating the direct pro-fibrotic effects of IL-17 (Figure 7b). In contrast, in the contact manner, the neutralisation of each cytokine (IL-17, IL-23 or IFN- $\gamma$ ) more or less inhibited liver fibrogenesis, with the neutralising anti-IL-17 Ab eliciting the strongest effect, collectively suggesting the pro-fibrotic effects of the axis, if present in the co-culture system, and IL-17 as the most downstream effector (Figure 7c). Meanwhile, in the single culture system, pHSCs were also treated with neutralising anti-IL-17, anti-IL-23 or anti-IFN- $\gamma$  Ab, and statistical data demonstrated that only the neutralisation of IFN- $\gamma$  showed pro-fibrogenic effects, confirming the anti-fibrogenic role of IFN- $\gamma$  in an autocrine manner (Supplementary figure 4e). Taken together, the 'anti-fibrotic' IFN- $\gamma$  may exert major effects as an upstream regulator of the 'pro-fibrotic' axis.

Because IFN- $\gamma$  can facilitate HSCs to acquire the phenotype of APCs, as demonstrated by the expression of molecules involved in antigen presentation (MHC-II, CD1d and CD1b) and T-cell activation (CD80, CD86),<sup>9,10</sup> while IL-23 is mainly produced by APCs,<sup>18,19</sup> IFN- $\gamma$  was suspected to exist as an upstream regulator of IL-23 production by pHSCs. As expected, contact co-culture with CD161<sup>+</sup>CD4<sup>+</sup> T cells, comparable to 500 U mL<sup>-1</sup> IFN- $\gamma$ , significantly enhanced the APC phenotype of pHSCs, as reflected by increased mRNA levels of CD80, CD86, MHC-II and CD1d, which was diminished by the neutralisation of IFN- $\gamma$  (Figure 7d). Flow cytometry was also performed to confirm the phenotypic characteristics of APCs in IFN- $\gamma$ -treated pHSCs (Supplementary figure 4g). Notably, contact co-cultures with CD161<sup>+</sup>CD4<sup>+</sup> T cells as compared to IFN- $\gamma$  had a much greater ability to induce IL-23 expression by pHSCs, which could be partly downregulated by the neutralising anti-IFN- $\gamma$  Ab, suggesting a mechanism besides IFN- $\gamma$  for IL-23 production (Figure 7d). Subsequently, the IL-23/IL-17 axis was confirmed by treating homologous CD161<sup>+</sup>CD4<sup>+</sup> T cell and CD161<sup>-</sup>CD4<sup>+</sup> T cells from the LC cohort ( $n = 6$ ) in the presence or absence of recombinant IL-23 for further analysis of IL-17 production in the supernatant. As shown in Figure 7e, rIL-23 showed dose-dependent effects in triggering IL-17 production by CD161<sup>+</sup>CD4<sup>+</sup> T

cells rather than CD161<sup>-</sup>CD4<sup>+</sup> T cells, demonstrating the requirement of CD161 signalling in the IL-23/IL-17 axis. In addition, IL-17 also exhibited dose-dependent effects in promoting liver fibrogenesis by pHSCs (Figure 7f). To date, the regenerative and pro-fibrotic IFN- $\gamma$ /IL-23/IL-17 axis has been established in the contact culture of CD161<sup>+</sup>CD4<sup>+</sup> T cell subsets with pHSCs.

### Evidence of direct contact between CD161<sup>+</sup> and $\alpha$ -SMA<sup>+</sup> cells in HBV-mediated cirrhotic livers

To obtain further evidence of direct contact between intrahepatic CD161<sup>+</sup>CD4<sup>+</sup> T cells and HSCs, the expression of lectin-like transcript 1 (LLT1, the ligand for CD161) was first determined in pHSCs and cirrhotic livers. Significantly elevated expression levels of LLT1 were observed not only in culture-activated vs. quiescent pHSCs (Supplementary figure 4b and c), but also in cirrhotic vs. normal livers (Figure 8a). In addition, there was a positive correlation between intrahepatic LLT1 and  $\alpha$ -SMA expression in cirrhotic livers (Figure 8b). Further, by immunohistochemical double staining of  $\alpha$ -SMA/CD161 and CD161/LLT1, both the spatial contacts and the remarkably increased area of positive co-staining were documented in cirrhotic livers, suggesting that CD161<sup>+</sup> cells may directly interact with HSCs to be involved in liver fibrogenesis (Figure 8c and d). Moreover, immunofluorescent triple staining of CD161/IL-23R/ $\alpha$ -SMA revealed a significant increase in  $\alpha$ -SMA<sup>+</sup> in direct contact with CD161<sup>+</sup>IL-23R<sup>+</sup> (being responsive to IL-23 for IL-17 production) cells in cirrhotic livers compared to normal livers (Figure 8e).

## DISCUSSION

The present study has elucidated several aspects of CD161<sup>+</sup>CD4<sup>+</sup> T cells in HBV-mediated pathogenesis: CD161<sup>+</sup>CD4<sup>+</sup> T cells accumulate in both peripheral and intrahepatic compartments, which produce abundant IL-17 and IFN- $\gamma$ , and express high levels of liver-homing chemokine receptors, including CCR6, CXCR6 and CX3CR1. Higher baseline and expanded numbers of circulating CD161<sup>+</sup>CD4<sup>+</sup> T cells were associated with an improved serological response of HBeAg to entecavir treatment. *In vitro*, CD161<sup>+</sup>CD4<sup>+</sup> T cells could enhance the pro-fibrogenic features of HSCs through the regenerative IFN- $\gamma$ /IL-23/IL-17 axis.

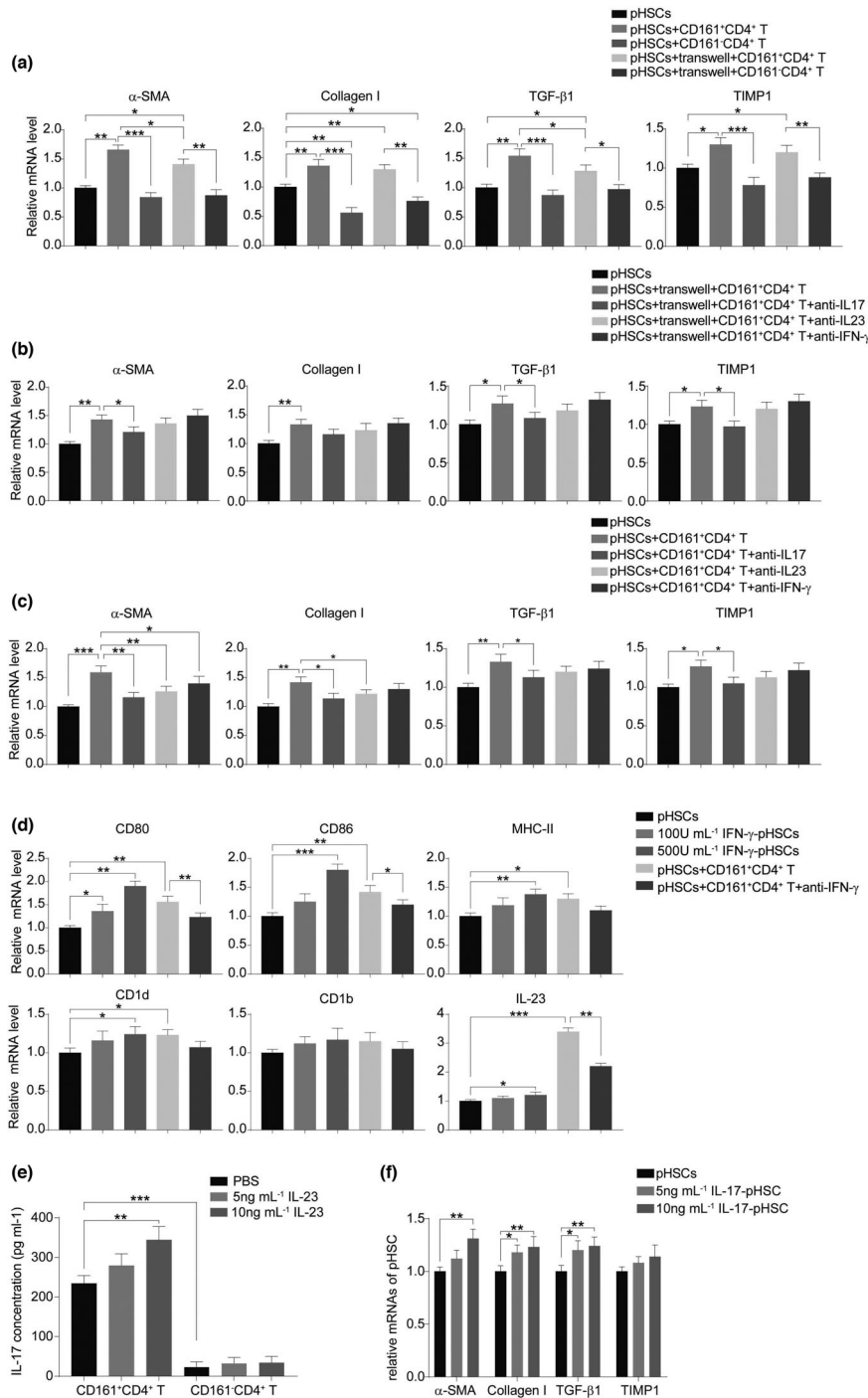


**Figure 7.** The pro-fibrogenic features of circulating CD161<sup>+</sup>CD4<sup>+</sup> T cells in chronic HBV settings. **(a–c)** Human pHSCs were co-cultured with circulating CD4<sup>+</sup> T subsets from LC cohort ( $n = 6$ ) at a cell-to-cell ratio of 1:1 for 72 h. After co-cultures, adherent pHSCs were collected for qRT-PCR analysis of genes involved in liver fibrogenesis including  $\alpha$ -SMA, collagen I, TGF- $\beta$ 1 and TIMP1. **(a)** Co-cultures with circulating CD161<sup>+</sup>CD4<sup>+</sup> T cells or homologous CD161<sup>-</sup>CD4<sup>+</sup> T cells in the contact or transwell manner. **(b, c)** Co-cultures with CD161<sup>+</sup>CD4<sup>+</sup> T cells in the transwell **(b)** or contact **(c)** manner in the presence or absence of neutralising anti-IL-17, anti-IL-23 or anti-IFN- $\gamma$  Ab. **(d)** pHSCs were stimulated with IFN- $\gamma$  or co-cultured with circulating CD161<sup>+</sup>CD4<sup>+</sup> T cells from LC cohort ( $n = 4$ ) in the presence or absence of the neutralising anti-IFN- $\gamma$  Ab. After 72 h, pHSCs were collected for qRT-PCR analysis of the APCs phenotypic markers of CD80, CD86, MHC-II, CD1d, CD1b and IL-23. **(e)** Homologous CD161<sup>+</sup>CD4<sup>+</sup> T cells and CD161<sup>-</sup>CD4<sup>+</sup> T cells from the circulation of LC cohort ( $n = 6$ ) were, respectively, treated with recombinant IL-23 at different concentrations for 72 h. Supernatant samples were collected to determine IL-17 concentration by ELISA. **(f)** pHSCs were treated with recombinant IL-17 at different concentrations for 72 h to be determined by qRT-PCR analysis of fibrosis markers (\* $P < 0.05$ ; \*\* $P < 0.01$ ; \*\*\* $P < 0.001$ ).

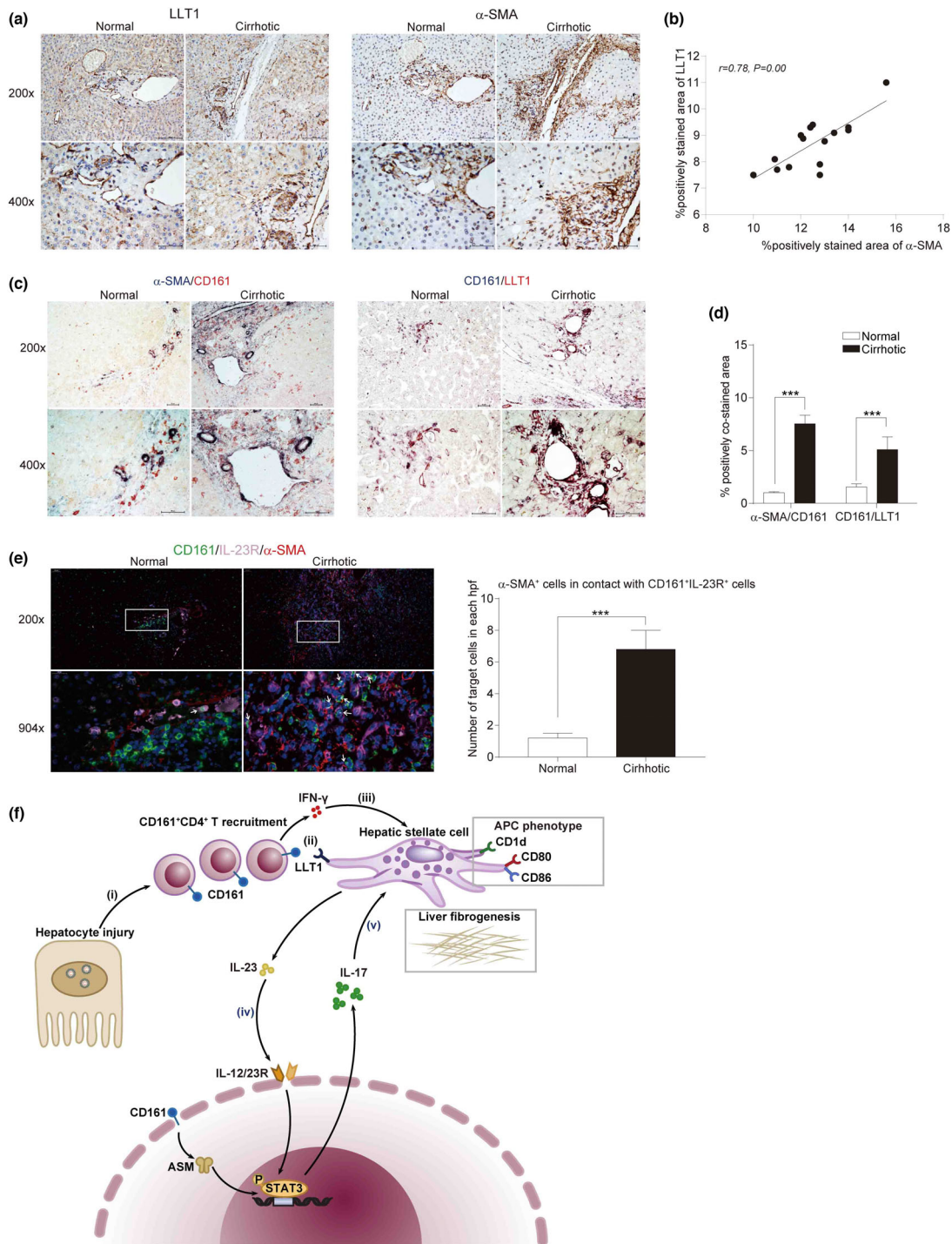


**Figure 8.** Evidence of direct contacts between CD161<sup>+</sup> and α-SMA<sup>+</sup> cells in HBV-mediated cirrhotic livers. **(a, b)** Representative immunohistochemical staining **(a)** and statistical correlation **(b)** of intrahepatic LLT1 and α-SMA in HHA and HCC cohorts (both *n* = 15). **(c, d)** Representative immunohistochemical co-staining **(c)** and quantification **(d)** of α-SMA/CD161 and CD161/LLT1 in HHA and HCC cohorts (both *n* = 6). **(e)** Representative colocalisation (left panel, white arrows indicate direct contact of CD161<sup>+</sup>IL-23R<sup>+</sup> with α-SMA<sup>+</sup> cells) and quantification (right panel) of CD161/IL-23R/α-SMA in HHA and HCC cohorts (both *n* = 6). **(f)** Working model of interactions between CD161<sup>+</sup>CD4<sup>+</sup> T cells and HSCs in chronic HBV infection: (i) HBV-associated liver injury induces recruitment of circulating CD161<sup>+</sup>CD4<sup>+</sup> T cells; (ii) ligation of CD161 by LLT1 (on HSCs) induces IFN-γ production by CD161<sup>+</sup>CD4<sup>+</sup> T cells; (iii) IFN-γ enhances the APC phenotype and IL-23 production in HSCs; (iv) IL-23 binds to its receptor IL-12R/IL-23R on CD161<sup>+</sup>CD4<sup>+</sup> T cells to promote IL-17 production; (v) IL-17 facilitates liver fibrogenesis in HSCs (\*\*\**P* < 0.001).

Statistical analysis of the frequencies of circulating CD161<sup>+</sup>CD4<sup>+</sup> T cells based on disease parameters, including hepatocellular injury (ALT and AST), viral replication (HBV DNA) and liver fibrosis progression (liver stiffness), showed that CD161<sup>+</sup>CD4<sup>+</sup> T cells are pro-inflammatory, antiviral and pro-fibrogenic in HBV-related pathogenesis. There are at least two reasons for their versatile roles in chronic HBV infection. First, CD161<sup>+</sup>CD4<sup>+</sup> T cells contain various functional subsets, as demonstrated by the diversity in both intracellular cytokines and chemokine receptors. Secondly, different activation mechanisms may play a role. Although CD161 has been identified as a co-stimulatory molecule in the context of T-cell receptor (TCR) stimulation, the TCR-independent production of IFN- $\gamma$  by CD161-expressing T cells has been described,<sup>7</sup> suggesting a bystander or unconventional activation pathway of CD161<sup>+</sup>CD4<sup>+</sup> T cells. However, our knowledge of antigen-specific CD161<sup>+</sup>CD4<sup>+</sup> T cells has been greatly restricted by the scarcity of cells. Future studies should focus on analysing CD161<sup>+</sup>CD4<sup>+</sup> T cells using pMHCII tetramer technology. To determine whether the documented disease correlations were HBV-specific, non-HBV cohorts of patients with chronic hepatitis (CH) were also analysed. The frequencies showed a similar increase in the circulation of non-HBV cohorts (Supplementary figure 3a); however, they failed to exhibit a correlation with clinical parameters (data not shown), suggesting an insignificant role in disease pathogenesis. In addition, CD161<sup>+</sup>CD4<sup>+</sup> T cells in CH conditions expressed much higher levels of pro-inflammatory cytokines, including IL-17A, IFN- $\gamma$  and IL-22 (Supplementary figure 3b and c), thus mediating inflammatory responses. In addition, CD161<sup>+</sup>CD4<sup>+</sup> T cells were enriched in HCV-infected livers with antiviral and hepatoprotective roles by co-expressing IL-17 and IL-22.<sup>2,4,20</sup> Taken together, CD161<sup>+</sup>CD4<sup>+</sup> T cells may have a more prominent role in viral hepatitis; however, their non-specific pro-inflammatory features could be extended to CH with non-HBV aetiologies.

Although CD161<sup>+</sup>CD8<sup>+</sup> T cells have been described to be critical for HBV control,<sup>2,3</sup> the role of CD161<sup>+</sup>CD4<sup>+</sup> T cells in anti-HBV immunity has not been determined. In this study, the circulating CD161<sup>+</sup>CD4<sup>+</sup> T frequencies were initially observed to be higher in HBeAg<sup>-</sup>CHB patients than in HBeAg<sup>+</sup>CHB patients and correlated better with disease parameters. This suggests that CD161<sup>+</sup>CD4<sup>+</sup>

T cells may be involved in HBeAg seroconversion, an important reflection of host anti-HBV immunity. Here, CD161<sup>+</sup>CD4<sup>+</sup> T cells were analysed based on HBeAg seroconversion in a longitudinal cohort undergoing 52-week antiviral treatment. Data documented higher baseline and treatment-expanded CD161<sup>+</sup>CD4<sup>+</sup> T frequencies in the circulation of responders. Also, these cells, as compared to their counterparts from non-responders, showed the phenotype of being less exhausted and more proliferative, suggesting an enhanced antiviral capacity. These findings collectively demonstrate the participation of CD161<sup>+</sup>CD4<sup>+</sup> T cells in HBeAg seroconversion. Although CD161<sup>+</sup>CD4<sup>+</sup> T cells lack direct cell-killing ability, they can mediate antiviral responses by helping CD8<sup>+</sup> T cells, or by producing a large amount of IFN- $\gamma$ , which has been described as an important mediator controlling intrahepatic pathogens.<sup>21</sup> Because CD161-expressing MAIT cells have recently been highlighted for the antiviral role<sup>22</sup> and our gating strategy of CD161<sup>+</sup>CD4<sup>+</sup> T cells could not entirely exclude MAIT cells (CD161<sup>+</sup>V $\alpha$ 7.2<sup>+</sup>), we investigated whether the antiviral effects of CD161<sup>+</sup>CD4<sup>+</sup> T cells were mediated by CD4<sup>+</sup>MAIT, which was then determined by the co-expression of V $\alpha$ 7.2 by CD161<sup>+</sup>CD4<sup>+</sup> T cells from HBV cohorts. The percentage of MAIT in CD161<sup>+</sup>CD4<sup>+</sup> T cells was rather low in both circulating and intrahepatic compartments (Supplementary figure 1j and k), which is consistent with previous studies.<sup>23,24</sup> These findings greatly reduced the possibility for CD4<sup>+</sup>MAIT subsets to play an antiviral role in chronic HBV infection. However, the discrepancy between MAIT and non-MAIT subsets in CD161<sup>+</sup>CD4<sup>+</sup> T cells should be explored in further investigations.

In patients with CHB, the phenotypic comparison between circulating CD161<sup>+</sup>CD4<sup>+</sup> T and homologous CD161<sup>-</sup>CD4<sup>+</sup> T cells has linked CD161 expression with a pro-inflammatory and liver-homing phenotype. However, CD161<sup>+</sup>CD4<sup>+</sup> T cells are exclusively memory cells, while CD161<sup>-</sup>CD4<sup>+</sup> T cells contain a mix of naïve and memory cells, which may simply reflect the differences between naïve and memory T cells. Additionally, subset analysis has suggested a close correlation between CXCR6 expression and the production of IFN $\gamma$ /IL-17 by CD161<sup>+</sup>CD4<sup>+</sup> T cells, since the most significant associations with HBV-related disease parameters have been documented in both CXCR6<sup>+</sup> and IFN- $\gamma$ <sup>+</sup>IL-17<sup>+</sup> subsets. Flow

cytometric co-staining of CD4/CD161/CXCR6/IFN- $\gamma$ /IL-17 was performed using PBMCs from CHB patients ( $n = 10$ ). The results indicated that the co-expression of IFN $\gamma$ /IL-17 by CXCR6<sup>+</sup>CD161<sup>+</sup>CD4<sup>+</sup> T cells was less than 3%, whereas almost all IFN- $\gamma$ <sup>+</sup>IL-17<sup>+</sup>CD161<sup>+</sup>CD4<sup>+</sup> T cells expressed CXCR6 (data not shown). Collectively, CXCR6 may be a major chemokine receptor that mediates liver infiltration of IFN- $\gamma$ <sup>+</sup>IL-17<sup>+</sup> subsets; however, the co-production of IFN- $\gamma$ /IL-17 is not a major characteristic of CXCR6<sup>+</sup> subsets.

If an accumulation of intrahepatic CD161<sup>+</sup>CD4<sup>+</sup> T cells occurs in HBV-infected patients, there may be potential connections between circulating and intrahepatic CD161<sup>+</sup>CD4<sup>+</sup> T cells. Intrahepatic CD161<sup>+</sup>CD4<sup>+</sup> T cells are more important than their circulating counterparts because they are directly involved in HBV-related liver injury and fibrosis progression. Because liver biopsy specimens are too small to obtain enough cells for flow cytometric analysis, surgical HCC and HHA cohorts were established to collect the paired specimens. To begin, an enrichment of both CD161<sup>+</sup>CD4<sup>+</sup> T cells and IFN- $\gamma$  and IL-17 co-expressing subsets was documented in cirrhotic livers as compared to normal livers. However, the correlation coefficients of total CD161<sup>+</sup>CD4<sup>+</sup> T cells and subsets from paired samples indicated that not all circulating CD161<sup>+</sup>CD4<sup>+</sup> T cells, but certain subsets will conduct trans-endothelial liver infiltration and participate in disease progression. Our data preliminarily suggest that IFN- $\gamma$  and IL-17 co-expressing subsets may probably migrate from the circulation. There are two mechanisms responsible for the increased number of intrahepatic CD161<sup>+</sup>CD4<sup>+</sup> T cells in disease conditions: liver recruitment through interactions between chemokine receptors and chemokines, and *in situ* proliferation. Here, our data demonstrated the interactions of CCR6/CCL20, CXCL16/CXCR6 and CX3CL1/CX3CR1 in liver recruitment of circulating CD161<sup>+</sup>CD4<sup>+</sup> T cells in chronic HBV infection, as supported by the following evidence: (1) The frequencies of circulating CD161<sup>+</sup>CD4<sup>+</sup> T subsets expressing chemokine receptors correlated better with disease parameters, in comparison with total CD161<sup>+</sup>CD4<sup>+</sup> T cells; (2) the correlation coefficients of the paired chemokine receptor-expressing subsets were much higher than those of total CD161<sup>+</sup>CD4<sup>+</sup> T cells; (3) the increased expression of chemokines in cirrhotic livers correlated with elevated numbers of intrahepatic CD161<sup>+</sup>CD4<sup>+</sup> T cells; (4) the spatial direct contacts

of chemokines with CD161<sup>+</sup> cells were documented to be enhanced in cirrhotic livers than in normal livers. However, most of the findings were based on carcinogenesis-associated cirrhosis, while cirrhosis in non-cancerous conditions might exhibit in a different way. Future studies should be conducted using non-cancerous cirrhotic samples.

To our knowledge, this study is the first to describe the regenerative IFN- $\gamma$ /IL-23/IL-17 axis between CD161<sup>+</sup>CD4<sup>+</sup> T cells and HSCs. The detailed working model is shown in Figure 8f. It is seemingly inexplicable that CD161<sup>+</sup>CD4<sup>+</sup> T cells produce abundant 'anti-fibrogenic' IFN- $\gamma$  but exert 'pro-fibrogenic' effects in the co-culture system. However, IFN- $\gamma$  was demonstrated not to directly regulate liver fibrogenesis by HSCs, but instead enhanced the APC phenotype of pHSCs to produce IL-23, which can further boost IL-23R<sup>+</sup>CD161<sup>+</sup>CD4<sup>+</sup> T cells to produce IL-17, which is the main effector that exerts pro-fibrogenic effects. The maximum liver fibrogenesis documented in the contact co-cultures indicates that the regenerability of the axis might require direct contact between CD161<sup>+</sup>CD4<sup>+</sup> T cells and HSCs, which are mainly mediated by membrane proteins, such as CD161/LLT1 engagement, which enhances IFN- $\gamma$  production by T cells.<sup>17</sup> To support the *in vivo* existence of the axis, LLT1 expression was upregulated in both activated HSCs and cirrhotic livers, while CD161<sup>+</sup>CD4<sup>+</sup> T subsets expressing IL-17, IFN- $\gamma$  or both were enriched in cirrhotic livers. Moreover, the spatial contacts between intrahepatic CD161<sup>+</sup>CD4<sup>+</sup> T cells and HSCs were confirmed by immunohistochemical double staining and immunofluorescent triple staining. In addition, similar pro-fibrogenic effects of the axis have been documented in cirrhotic patients with non-HBV aetiologies (Supplementary figure 4f); however, further *ex vivo* evidence of intrahepatic direct contact between HSCs and CD161<sup>+</sup>CD4<sup>+</sup> T cells is needed to demonstrate non-HBV specificity of the axis, which is beyond the scope of this study. Collectively, CD161<sup>+</sup>CD4<sup>+</sup> T cells could enhance liver fibrogenesis by HSCs via the regenerative IFN- $\gamma$ /IL-23/IL-17 axis in chronic HBV infection.

In summary, CD161<sup>+</sup>CD4<sup>+</sup> T cells play pro-inflammatory, antiviral and pro-fibrogenic roles in chronic HBV infection. These findings shed light on developing therapies targeting CD161<sup>+</sup>CD4<sup>+</sup> T cells to regulate HBV-related liver disease progression.

## METHODS

### Subjects

A total of 94 patients with CHB, 73 with HBV-mediated LC and 28 healthy controls (HC) were enrolled in this study. The phenotypic analysis of circulating CD161<sup>+</sup>CD4<sup>+</sup> T cells was carried out before antiviral treatment (clinical parameters of subjects are summarised in Supplementary table 1). As disease controls, chronic hepatitis and cirrhotic patients with non-HBV aetiologies including autoimmune, non-alcoholic steatohepatitis (NASH) and alcohol were also analysed. Of the HBV cohorts, HBeAg-positive patients (CHB,  $n = 50$ ; LC,  $n = 34$ ) were followed up for a period of 52-week entecavir monotherapy. At 3, 6, 9 and 12 months after treatment, the serological responses of HBeAg were evaluated. Here, responders were defined as those who achieved HBeAg seroconversion, referring to HBeAg loss with or without the appearance of anti-HBe antibody (Ab). The baseline characteristics of the responders and non-responders are summarised in Supplementary table 2. In addition, liver biopsy specimens from 62 patients with chronic HBV infection were also examined (Supplementary table 3). The degree of inflammation ('A' for activity) and fibrotic stage ('F' for fibrosis) were graded according to the Metavir scoring system by two senior pathologists.<sup>25</sup> The patients were diagnosed and classified as previously described.<sup>26</sup> The exclusion criteria for HBV cohorts included drug abuse, other viral infections, coexisting serious illness and pregnancy.

To explore discrepancies between circulating and intrahepatic CD161<sup>+</sup>CD4<sup>+</sup> T cells, 15 patients with HCC secondary to HBV-associated cirrhosis and 15 with surgery-requiring hepatic haemangioma (HHA) (clinical parameters summarised in Supplementary table 4) were enrolled to analyse the paired blood and liver samples. Here, cirrhotic and normal liver specimens were collected as tumor-free para-tumorous tissues (at least 1 cm away from the tumor) from HCC and HHA cohorts.

### Ethics statement

All individuals enrolled in this study provided written informed consent. The study protocol was approved by the Research Ethics Committee of Zhongshan Hospital (B2013-068, B2016-059) and Tongji Hospital (2015-KYSB-11).

### Reagents

For flow cytometry, anti-human antibodies (Abs) for CD3-percp-cy5.5 (SK7), CD161-Percp-cy5.5 (HP-3G10), CD45RO-PE (UCHL1), and IFN- $\gamma$ -PE (4S.B3), IL-17-APC (64DEC17), TNF- $\alpha$ -PE (MAb11), IL-22-eFlour450 (22URT1) and IL-10-PE (JES3-9D7) were purchased from eBioscience (Thermo Fisher Scientific, Waltham, USA). Antibodies against PD-1-BV510 (EH12.2H7), TIM-3-PE(F38-2E2), CD39-Percp-cy5.5 (A1), CTLA-4-PE (L3D10) and Ki-67-BV421 (Ki-67) were purchased from Biologend (San Diego, CA, USA). Antibodies against CD3-BV421 (SK7), CD4-BB515 (RPA-T4), CD161-APC (DX12), CD25-PE (M-A251), CCR6-PE-Cy7 (11A9), CXCR6-BV421 (13 B 1E5),

CX3CR1-PE (2A9-1), Foxp3-PE (236A/E7) and IL-4-Percp-Cy5.5 (8D4-8) were purchased from BD Biosciences. Stimulatory anti-CD161 antibody was purchased from BD Bioscience (Becton). Imipramine was purchased from Sigma-Aldrich (St. Louis, MO, USA), and recombinant human cytokine IL-23 (rIL-23) was purchased from R&D Systems (Bio-Techne, Minnesota).

### Preparation of circulating and intrahepatic cell samples

Peripheral blood mononuclear cells were isolated from ethylenediaminetetraacetic acid (EDTA)-treated blood samples (10 ml) using the Ficoll density gradient centrifugation method (GE Healthcare, USA). Circulating CD161<sup>+</sup>CD4<sup>+</sup> and CD161<sup>+</sup>CD4<sup>+</sup> T cells were sorted from PBMCs by FACS Aria II (Becton Dickinson) after sterile surface staining for CD3, CD4 and CD161, and the cell purity was confirmed to be > 95% (Supplementary figure 2a).

A single-cell suspension of mouse liver tissue was prepared using the gentle MACS Dissociator (Miltenyi Biotec) with subsequent digestion by collagenase type I (Sigma-Aldrich) and DNase (Gibco). Liver-infiltrating lymphocytes (LILs) were recovered by centrifugation over 40% and 70% Percoll gradient (GE Healthcare). Using peritumoral liver specimens from the HHA cohort ( $n = 5$ ), primary HSCs (pHSCs) were isolated through 8% Nycodenz (Axis-Shield) gradient centrifugation and then cultured in high-glucose DMEM supplemented with 10% FBS. The cell purity of HSCs was demonstrated by positive staining for  $\alpha$ -smooth muscle actin ( $\alpha$ -SMA) (Supplementary figure 4a).

### Flow cytometry

Peripheral blood mononuclear cells and LILs were prepared for phenotypic analysis of circulating and intrahepatic CD161<sup>+</sup>CD4<sup>+</sup> T cells. Human Fc Block™ (BD Bioscience, USA) was used to block non-specific binding. Dead cells were excluded using a fixable viability dye (FVD)-780 (eBioscience). Negative controls were set appropriately. FMO (fluorescence minus one) staining was performed to set a proper gate for indicators without an obvious bimodal distribution of expression. For staining of intracellular cytokines, cells were pre-treated with a cell stimulation cocktail containing phorbol-12-myristate-13-acetate (PMA) and ionomycin (2  $\mu$ L mL<sup>-1</sup>) (eBioscience) for 5 h. A minimum of  $1 \times 10^5$  cells were collected by LSRFortessa™ (BD Bioscience) for further analysis using FlowJo V10 software (Tree Star).

### Immunohistochemistry and immunofluorescence

For immunohistochemistry, liver tissue specimens (4  $\mu$ m, paraffin-embedded, formalin-fixed) were dewaxed, hydrated and subjected to heat-induced antigen retrieval. Sections were blocked with 5% BSA (Sigma-Aldrich). A standard two-step protocol (Novolink Polymer Detection System) was applied with the following primary antibodies: rabbit anti- $\alpha$ -SMA (1:1000) (ab124964), mouse anti-CD161 (1:200) (556079; BD Biosciences), rabbit anti-IL-23R (1:100) (ab175072), rabbit anti-

LLT1 (1:100) (ab197341), rabbit anti-CCL20 (1:100, ab136904), rabbit anti-CXCL16 (1:100, #500-P200, Peprotech) and rabbit anti-CX3CL1 (1:400) (ab89229). Immunohistochemical double staining was performed using a DouMaxVision™ kit (MXB). Immunofluorescence triple staining was performed by Servicebio Technology Co., Ltd (Wuhan, China). The positively stained area was quantified by ImageJ (NIH), while the number of positively stained cells was calculated using Image-Pro Plus version 6.0 (Media Cybernetics, Rockville, MD, USA). Six high-power fields (hpf, 400× magnification) of each specimen were selected for the statistical analysis.

## Cell cultures and co-cultures

T-cell activity was maintained *in vitro* using anti-CD3/CD28 beads at a bead-to-cell ratio of 1:1. At different cell ratios, pHSCs ( $5 \times 10^4$  per well in 24-well plates) were co-cultured with sorted circulating CD4<sup>+</sup> T subsets in the contact or non-contact manner for 72 h, with or without addition of the neutralising anti-IL-17 ( $10 \mu\text{g mL}^{-1}$ ) (AF-317-NA; R&D Systems), anti-IL-23p19 ( $100 \mu\text{g mL}^{-1}$ ) (AF1716; R&D Systems) or anti-IFN- $\gamma$  ( $50 \mu\text{g mL}^{-1}$ ) (MAB285; R&D Systems) Ab. The non-contact co-culture was carried out using a transwell system (Corning) with a polycarbonate membrane (pore size: 0.4  $\mu\text{m}$ , not allowing cells to pass through) between the upper and lower compartments.

## Quantitative reverse transcription PCR (qRT-PCR)

Approximately  $1 \times 10^5$  cells were collected for qRT-PCR analysis. Total RNA was extracted using Trizol (Invitrogen), followed by reverse transcription and quantitative real-time PCR using commercial kits (Takara Bio). The list of primers used are shown in Supplementary table 5. The mRNA levels were calculated using the  $\Delta\Delta\text{Ct}$  method after normalisation with GAPDH and quantified as fold change.

## Detection of cytokines in supernatants

To determine *in vitro* cytokine production, supernatant samples were collected after treating cells (a total of  $1 \times 10^6$ ) with anti-CD3/CD28 beads at a bead-to-cell ratio of 1:1 for 72 h. CBA analysis was then applied to detect cytokine concentrations using the commercial Human Th Cytokine Panel kit (IFN- $\gamma$ /TNF- $\alpha$ /IL-17/IL-21/IL-22, LEGENDplex™; Biolegend) and LSRFortessa™. The concentration of IL-17 was also analysed using a human enzyme-linked immunosorbent assay (ELISA) kit (eBioscience).

## Western blot analysis

Approximately  $1 \times 10^5$  cells were collected for cell lysis, protein extraction and western blot analysis. PhosSTOP (Roche) was added before analysing the phosphorylated forms of the proteins. Protein levels were assessed using primary rabbit anti-human Abs: STAT3 (88 kDa) (10253-2-AP; Proteintech), phospho-STAT3 at Tyr<sup>705</sup> (79, 86k Da) (#9145; CST) and LLT1 (34 kDa) (ab151738; Abcam). Relative protein expression was normalised with an anti- $\beta$ -actin

antibody (42 kDa) (Proteintech) and quantified using ImageJ (NIH).

## Statistical analysis

Results are presented as the mean  $\pm$  SD or mean (range). Statistical analyses were performed using GraphPad Prism version 7.0 (San Diego, CA, USA). The Student's *t*-test, analysis of variance (ANOVA) with the Bonferroni test and the Pearson correlation analysis were performed as appropriate. Statistical significance was set at  $P \leq 0.05$ .

## ACKNOWLEDGMENTS

This study was supported by grants from the National Natural Science Foundation of China (grant no. 81670541 to Wei Jiang, 81670571 and 818201008006 to YCQ, 81570513 to LJ and 81900545 to CLS), National Major Science and Technology Project (2013ZX10002004 and 2017ZX10203202003002 to JW), National Key Technologies R&D Program (2015BAI13B09 to JW), Xiamen Medical and Health Guidance Project (3502Z20199177 to JW) and Xiamen Superior Subspecialty Construction Project, Shanghai Municipal Health Commission 'Outstanding Youth Medical Talent Training Program' (2017YQ025 to LJ), Shanghai Municipal Science and Technology Commission 'Western Medicine Guidance Project' (17411970600 to LJ) and Shanghai Municipal Key Specialty Project (no. Shslczdzk06801 to YCQ). We also acknowledge the contribution of Binghua Dai (Department of Liver Transplantation & Special Treatment, Eastern Hepatobiliary Surgery Hospital, The Second Military Medical University, Shanghai, China) in the collection of surgical liver samples.

## CONFLICT OF INTEREST

The authors declare no conflict of interest.

## AUTHOR CONTRIBUTIONS

**Wei Jiang:** Conceptualization; Funding acquisition; Project administration; Supervision. **Jing Li:** Conceptualization; Data curation; Formal analysis; Funding acquisition; Investigation; Writing-original draft; Writing-review & editing. **Lisha Cheng:** Conceptualization; Data curation; Formal analysis; Funding acquisition; Writing-original draft. **Haoyu Jia:** Data curation; Formal analysis; Resources. **Chun Liu:** Data curation; Methodology. **Siqi Wang:** Data curation. **Yun Liu:** Data curation. **Yue Shen:** Data curation. **Shengdi Wu:** Methodology. **Fanli Meng:** Methodology. **Beishi Zheng:** Methodology. **Changqing Yang:** Conceptualization; Funding acquisition; Supervision.

## REFERENCES

- Cheng LS, Liu Y, Jiang W. Restoring homeostasis of CD4<sup>+</sup> T cells in hepatitis-B-virus-related liver fibrosis. *World J Gastroenterol* 2015; 21: 10721–10731.



2. Northfield JW, Kasprovicz V, Lucas M et al. CD161 expression on hepatitis C virus-specific CD8<sup>+</sup> T cells suggests a distinct pathway of T cell differentiation. *Hepatology* 2008; **47**: 396–406.
3. Billerbeck E, Kang YH, Walker L et al. Analysis of CD161 expression on human CD8<sup>+</sup> T cells defines a distinct functional subset with tissue-homing properties. *Proc Natl Acad Sci USA* 2010; **107**: 3006–3011.
4. Bolte FJ, O'Keefe AC, Webb LM et al. Intra-hepatic depletion of mucosal-associated invariant T cells in hepatitis C virus-induced liver inflammation. *Gastroenterology* 2017; **153**: 1392–1403.e2.
5. Boeijen LL, Montanari NR, de Groen RA et al. Mucosal-associated invariant T cells are more activated in chronic hepatitis B, but not depleted in blood: reversal by antiviral therapy. *J Infect Dis* 2017; **216**: 969–976.
6. Cosmi L, De Palma R, Santarasci V et al. Human interleukin 17-producing cells originate from a CD161<sup>+</sup>CD4<sup>+</sup> T cell precursor. *J Exp Med* 2008; **205**: 1903–1916.
7. Fergusson JR, Smith KE, Fleming VM et al. CD161 defines a transcriptional and functional phenotype across distinct human T cell lineages. *Cell Rep* 2014; **9**: 1075–1088.
8. Tsuchida T, Friedman SL. Mechanisms of hepatic stellate cell activation. *Nat Rev Gastroenterol Hepatol* 2017; **14**: 397–411.
9. Winau F, Hegasy G, Weiskirchen R et al. Ito cells are liver-resident antigen-presenting cells for activating T cell responses. *Immunity* 2007; **26**: 117–129.
10. Viñas O, Bataller R, Sancho-Bru P et al. Human hepatic stellate cells show features of antigen-presenting cells and stimulate lymphocyte proliferation. *Hepatology* 2003; **38**: 919–929.
11. Yu MC, Chen CH, Liang X et al. Inhibition of T-cell responses by hepatic stellate cells via B7-H1-mediated T-cell apoptosis in mice. *Hepatology* 2004; **40**: 1312–1321.
12. Jiang G, Yang HR, Wang L et al. Hepatic stellate cells preferentially expand allogeneic CD4<sup>+</sup>CD25<sup>+</sup>FoxP3<sup>+</sup> regulatory T cells in an IL-2-dependent manner. *Transplantation* 2008; **86**: 1492–1502.
13. Chinnadurai R, Grakoui A. B7–H4 mediates inhibition of T cell responses by activated murine hepatic stellate cells. *Hepatology* 2010; **52**: 2177–2185.
14. Li J, Qiu SJ, She WM et al. Significance of the balance between regulatory T (Treg) and T helper 17 (Th17) cells during hepatitis B virus related liver fibrosis. *PLoS One* 2012; **7**: e39307–e39319.
15. Li J, Wang FP, She WM et al. Enhanced high-mobility group box 1 (HMGB1) modulates regulatory T cells (Treg)/T helper 17 (Th17) balance via toll-like receptor (TLR)-4-interleukin (IL)-6 pathway in patients with chronic hepatitis B. *J Viral Hepat* 2014; **21**: 129–140.
16. Li J, Jia M, Liu Y et al. Telbivudine therapy may shape CD4<sup>+</sup> T-cell response to prevent liver fibrosis in patients with chronic hepatitis B. *Liver Int* 2015; **35**: 834–845.
17. Bai A, Guo Y. Acid sphingomyelinase mediates human CD4<sup>+</sup> T-cell signaling: potential roles in T-cell responses and diseases. *Cell Death Dis* 2017; **8**: e2963–e2969.
18. Wang Q, Zhou J, Zhang B et al. Hepatitis B virus induces IL-23 production in antigen presenting cells and causes liver damage via the IL-23/IL-17 axis. *PLOS Pathog* 2013; **9**: e1003410–e1003424.
19. McGeachy MJ, Chen Y, Tato CM et al. The interleukin 23 receptor is essential for the terminal differentiation of interleukin 17-producing effector T helper cells *in vivo*. *Nat Immunol* 2009; **10**: 314–324.
20. Kang YH, Seigel B, Bengsch B et al. CD161<sup>+</sup>CD4<sup>+</sup> T cells are enriched in the liver during chronic hepatitis and associated with co-secretion of IL-22 and IFN- $\gamma$ . *Front Immunol* 2012; **3**: 346.
21. Wang J, Holmes TH, de Guevara LL et al. Phenotypic and functional status of intrahepatic T cells in chronic hepatitis C. *J Infect Dis* 2006; **194**: 1068–1077.
22. Van Wilgenburg B, Scherwitzl I, Hutchinson EC et al. MAIT cells are activated during human viral infections. *Nat Commun* 2016; **7**: 11653.
23. Kurioka A, Jahun AS, Hannaway RF et al. Shared and distinct phenotypes and functions of human CD161<sup>++</sup>V $\alpha$ 7.2<sup>+</sup> T cell subsets. *Front Immunol* 2017; **8**: 1031.
24. Gherardin NA, Souter MN, Koay HF et al. Human blood MAIT cell subsets defined using MR1 tetramers. *Immunol Cell Biol* 2018; **96**: 507–525.
25. Bedossa P, Poynard T. An algorithm for the grading of activity in chronic hepatitis C. The METAVIR Cooperative Study Group. *Hepatology* 1996; **24**: 289–293.
26. EASL, European Association for the Study of the Liver. EASL 2017 Clinical Practice Guidelines on the management of hepatitis B virus infection. *J Hepatol* 2017; **67**: 370–398.

## Supporting Information

Additional supporting information may be found online in the Supporting Information section at the end of the article.



This is an open access article under the terms of the Creative Commons Attribution-NonCommercial-NoDeriv License, which permits use and distribution in any medium, provided the original work is properly cited, the use is non-commercial and no modifications or adaptations are made.